Article

Field-Induced Single Molecule Magnetic Behavior of Mononuclear Cobalt(II) Schiff Base Complex Derived from 5-Bromo Vanillin

Fikre Elemo [1,2], Sören Schlittenhardt [3], Taju Sani [1,2], Cyril Rajnák [4], Wolfgang Linert [5], Roman Boča [4], Madhu Thomas [1,2,*] and Mario Ruben [3,6,7,*]

1   Department of Industrial Chemistry, College of Applied Science, Addis Ababa Science and Technology University, Addis Ababa P.O. Box 16417, Ethiopia; fikre.elemo@aastu.edu.et (F.E.); taju.sani@aastu.edu.et (T.S.)
2   Nanotechnology Centre of Excellence, Addis Ababa Science and Technology University, Addis Ababa P.O. Box 16417, Ethiopia
3   Institute of Nanotechnology, Karlsruhe Institute of Technology, Hermann-von-Helmholtz-Platz 1, D-76344 Eggenstein-Leopoldshafen, Germany; soeren.schlittenhardt@kit.edu
4   Department of Chemistry, Faculty of Natural Sciences, University of SS Cyril and Methodius, 91701 Trnava, Slovakia; cyril.rajnak@ucm.sk (C.R.); roman.boca@ucm.sk (R.B.)
5   Institute of Applied Physics, Vienna University of Technology, Wiedner Hauptstraße 8-10, 1040 Vienna, Austria; wolfgang.linert@tuwien.ac.at
6   Institute for Quantum Materials and Technologies, Karlsruhe Institute of Technology, Hermann-von-Helmholtz-Platz 1, D-76344 Eggenstein-Leopoldshafen, Germany
7   Centre Européen de Science Qantique (CESQ), Institut de Science et d'Ingénierie Supramoléculaires (ISIS, UMR 7006), CNRS-Université de Strasbourg, 8 Allée Gaspard Monge, BP 70028, CEDEX, F-67083 Strasbourg, France
*   Correspondence: madhu.thomas@aastu.edu.et (M.T.); mario.ruben@kit.edu (M.R.)

Abstract: A mononuclear Co(II) complex of a Schiff base ligand derived from 5-Bromo-vanillin and 4-aminoantipyrine, that has a compressed tetragonal bipyramidal geometry and exhibiting field-induced slow magnetic relaxation, has been synthesized and characterized by single crystal X-ray diffraction, elemental analysis and molecular spectroscopy. In the crystal packing, a hydrogen-bonded dimer structural topology has been observed with two distinct metal centers having slightly different bond parameters. The complex has been further investigated for its magnetic nature on a SQUID magnetometer. The DC magnetic data confirm that the complex behaves as a typical $S = 3/2$ spin system with a sizable axial zero-field splitting parameter $D/hc = 38$ cm^{-1}. The AC susceptibility data reveal that the relaxation time for the single-mode relaxation process is $\tau = 0.16(1)$ ms at $T = 2.0$ K and $B_{DC} = 0.12$ T.

Keywords: Schiff base; slow relaxation; molecular spectroscopy; packing; zero-field

1. Introduction

Single-molecule and single-ion magnets (SMMs, SIMs), realized in transition metal complexes showing slow magnetic relaxation, have gained much attention in molecular magnetism. These types of compounds are applicable in various technological areas such as switches, sensors, displays, low-temperature magnetic refrigerators, high-density information storage devices and quantum computing [1–6]. They show characteristic magnetic properties, such as slow relaxation of magnetization due to magnetic bistability of two ± MS levels at a molecular level [7,8]. Arising from a bistable ground state and uniaxial anisotropy in SMMs, a non-zero magnetization of the compound can be retained upon the removal of an external field below its specific blocking temperature [8]. Due to this retained magnetization, even in the absence of an applied field, SMMs can be utilized in information storage at the molecular level or in spintronic devices [9–12].

Historically, SMMs of transition metals with polynuclear topology possessed a high spin ground state with magnetic anisotropy leading to an energy barrier to the reorientation of their magnetization [13–15]. Due to the structural complexity in polynuclear complexes, prediction of the magnetic anisotropy for enhancing the energy barrier and studying the stability in solution is becoming complicated and difficult [16–20]. Later, many works have been reported on mononuclear Schiff base single molecule (single-ion) magnets to overcome the complexity and difficulty [21,22]. Mononuclear single molecule magnets, so-called single ion magnets (SIMs), consist of a single paramagnetic center per molecule in a given ligand environment [23–25].

The d-block multinuclear complexes are probably not the best choice for obtaining higher effective energy barriers. Hence, the investigation of the d-block mononuclear chemistry is growing exponentially because the high magnetic anisotropy enhances the barrier to spin reversal. It is striking that few of these compounds reported to date are mononuclear magnets in the zero field [13–15,26]. The design of SIMs and SMMs is still a big challenge concerning the fundamental understanding of the origin of magnetic anisotropy and dynamic relaxation. Magnetic anisotropy achieved by strict regulation of geometry is the most critical factor for high-performance SMMs and SIMs [27], which is dependent on axial anisotropy (D), along with spin ground state (S) [28]. Designing the Schiff base ligand-field, which can preserve strict axial symmetry around the metal ion, is one of the best approaches to increase the zero-field splitting in d-metal mononuclear magnets. To do so, the design and synthesis of new ligands and the proper use of existing ones will remain at the fore [29–31].

Magnetic anisotropy, which is a defining feature of SIMs, can be enhanced by weak ligand fields, designing a molecule with a lower oxidation state, higher local symmetry and lower coordination number [14,19,32,33]. All these factors are important to obtaining 3d-based SMMs and SIMs because in 3d metals, the orbital angular momentum is readily quenched by the ligand field [14,34]. For mononuclear 3d metal compounds showing slow magnetic relaxation, a low coordination number which leads to a relatively weak Schiff base ligand field is needed because they reduce the 3d orbital splitting energy, thereby enhancing magnetic anisotropy [35–39]. In addition, this type of ligand can be well used as a coordinative moiety of transition metal complexes or as a building block for supramolecular assemblies by taking advantage of π-conjugation. In addition, these functional ligands can act as a bridge between different metal centers to give polynuclear complexes [40–42].

In transition metal-based mononuclear molecular magnetism, the ions are typically low-coordinate ions in the 2$^+$ and 3$^+$ oxidation states and are extremely Lewis acidic so that they can readily bind to nucleophiles (ligands) and can be directly bound to charge compensating atoms [43]. The majority of monometallic 3d molecular magnets are based on the half-integer spin of the metal ion, due to its ability to display slow relaxation of magnetization in a range of coordination environments [44]. Co (II) ions are interesting candidates among transition metal-based single-ion magnets because of their non-integer spin ground state, which decreases the probability of quantum tunneling of magnetization (QTM). Based on this argument, many low coordinate Co(II) single-molecule magnets of different coordination geometry were reported to date [32,45–47].

Magnetic anisotropy, which governs the barrier height for slow relaxation of magnetization, is the key factor in the design of SIM compounds. A negative D value results in uniaxial type magnetic anisotropy and a positive D value results in easy plane anisotropy, albeit only under an external magnetic field so-called field-induced SMM. The negative sign of D (easy axis) has advantages over the positive sign of D (easy plane), because the former energetically favors high $|m_S|$ states whereas the latter favors the $m_S = 0$ singlet for systems with integer S and the $m_S = \pm 1/2$ Kramer's doublet for those with half-integer S [48–53]. Since the spin is free to rotate within the easy plane, this may result in zero energy barriers unless there is some in-plane anisotropy. To overcome these phenomena, the potential chelating nature of the ligands on the cobalt geometry and its small bite angle would induce significant geometrical constraints at the metal center to retain magnetic anisotropy.

We are interested to give attention to a Co(II) complex because of its high-spin d^7 configuration, which is comfortable to generate large magnetic anisotropy with orbital contribution either by an orbitally degenerate ground state with unquenched orbital momentum by the crystal field or by the spin-orbit coupling when the orbital degeneracy is broken in a low-symmetry ligand field [54]. Herein, we present our investigations on a mononuclear Co (II) Schiff base complex showing field-induced slow magnetic relaxation.

2. Results and Discussion

2.1. Crystal Structure Description

The key structural features of the complex under study are summarized in Table S1. A perspective view of this complex with a selected atom-numbering scheme is shown in Figure 1. Single-crystal X-ray structure analysis revealed that the crystal structure consists of a mononuclear neutral molecule of $Co(C_{19}H_{17}BrN_3O_3)_2$ (**1**) with the molecular formula, $C_{38}H_{34}Br_2CoN_6O_6 \cdot 4(CH_3OH)$, which crystallizes in the monoclinic *Cc* space group (Figure 1 and Table S1). The cobalt in the structure occupies a special position with site symmetry 1 in the centrosymmetric space group. The symmetry is between the two molecules within the unit cell. This means that the asymmetric unit contains two compressed tetragonal bipyramidal complex molecules, each containing two ligands and one Co (II) ion in a coordination environment.
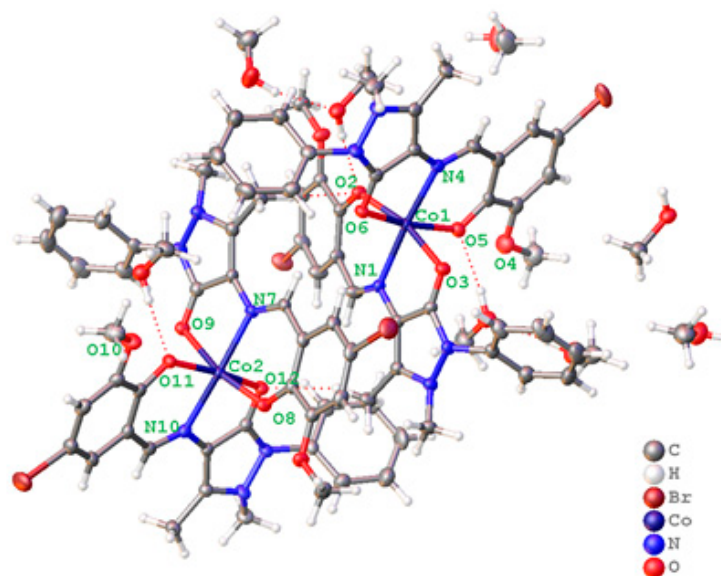
Figure 1. Single-crystal X-ray structure of **1** shown at 50% probability.

The four basal oxygen atoms and two nitrogen atoms, where both of the nitrogen atoms coordinated to the Co (II) center are from two identical coordinated ligands. The molecule crystallizes with four solvent (methanol) molecules in the coordination lattice. The non-coordinated methoxy oxygen acts as a hydrogen bond acceptor from adjacent groups and solvent molecules in the lattice.

There are two crystallographically distinct cobalt atoms Co1/Co2 (Figure 1) in the compound, but both have the same surroundings with very close bond lengths and angles. The cobalt (II) environment in both centers (Co1/Co2) complies with a compressed tetragonal bipyramidal of the {CoO$_4$N$_2$} group. The {CoN$_2$O$_4$} group possesses Co-O bond distances from 1.995(2) (Co2-O11) to 2.242(2) Å (Co2-O9) (Table S2), where four oxygen atoms from two ligands occupy the equatorial positions around the central Co (II) ion. The axial positions are occupied by two coordinated nitrogen atoms from the two ligands with the coordination distance of 2.079 Å for Co2-N7 and 2.092 Å for Co2-N10 in Co2 center as well as 2.087 Å for Co1-N1 and 2.086 Å for Co1-N4, respectively (Table S2). The dissimilarity in Co-N bond lengths in (Figure 1) is apparent that the coordination polyhedron

in the compound is much distorted because of the significant differences the significant differences found in the metal–ligand bond lengths. This can also be supported by the linear N-N distance of 4.169 Å in Co1, whereas 4.163 Å is in the Co2 center. All of the Co-O and the Co-N bond lengths of the molecule are in good agreement with the reported bond distances with high spin Co^{II} ions [36,55,56].

The bond distance of Co2-O11 1.995(2) Å and the Co2-O9 2.242(2) Å of the ligand are substantially the shortest and longest distances recorded in the molecule, respectively. The slight difference in the values of the cobalt-to-nitrogen bond lengths, which covers the maximum ranges of 2.079(2) Å (Co2-N7) to 2.092 Å (Co2-N10) in the Co2 center than the range 2.086 Å (Co1-N4) to 2.087 Å (Co1-N1) in the Co1, is indicative of the more asymmetric property in the Co1 center.

The deviation of angles of N10-Co2-O12 (82.05(2))° and N10-Co2-O11 (88.89(2))° as well as N7-Co2-O9 (80.99(9))° and N7-Co2-O8 (89.57(9))° in the Co2 center from the angle of an ideal octahedron (90°) is also further evidence for a greater angular distortion of the coordination center from the octahedral to a compressed tetragonal bipyramidal geometry.

The complex also contains non-covalent intermolecular interactions (hydrogen bonding and π-π interactions) between neighboring complex molecules, giving rise to the formation of a 2D network (Figure S1a,b), chain structures and a supramolecular three-dimensional structure (Figure S2a,b) through hydrogen bonding (Figure 2a) and π-π interactions between the rings (Figure 2b). The intermolecular hydrogen bond and π-π stacking interactions between coordinated ligand and solvent molecules in the lattice are linked to the neighboring molecules and result in the 2D network. This kind of interaction has the advantage to generate even polymers [57]. The noncovalent interactions in the cobalt complex have additional importance, which play a vital role in stabilizing the 2D and 3D network structures [58]. In the crystal lattice of the complex, the solvent molecules and some of the coordinated oxygen groups are efficient hydrogen bond donors, therefore, extensive hydrogen bonding is observed in the molecules. Two different hydrogen bonding modes appear in the molecule with shortest and longest bond distances. One is the intramolecular hydrogen bonds found with the equatorially coordinated oxygen atoms from the ligand to the solvent oxygen atom with the shortest bond distance of O-O, 2.605 Å. The second is with the methoxy oxygen atoms from the ligand to the solvent oxygen atom with the longest bond distance of O-O, 3.023 Å. These hydrogen bonds link the individual solvent molecules in the lattice to neighboring molecules resulting in infinite chains running along the b axis as in the close packing structure observed in Figure S2. The packing arrangement contains eight molecules of the complex in a unit cell.
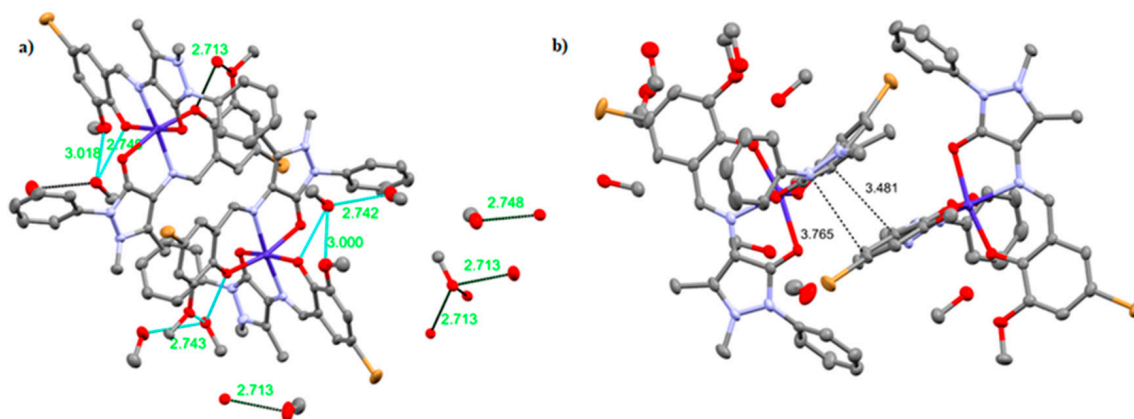
Figure 2. (**a**) Hydrogen bonding (**b**) π-π stacking interaction in **1**.

In addition to this, unconventional hydrogen bonding interactions are also observed in the molecule. These are the polar methanol solvents in the lattice and form strong self-hydrogen bonds with the shortest and longest bond distances of 2.716 Å and 3.010 Å, respectively (Figure 2a). The hydrogen atom of the methanol is involved in hydrogen-

bonding interactions with neighboring molecules, albeit with somewhat smaller contact distances in the range of 2.716 Å for connecting with the coordinated oxygen and in the range of 2.754 Å with non-coordinated methoxy oxygen of the o-vanillin entity. The observed H-bonding and π-π stacking in the molecule played a vital role in governing the architecture of the structure by generating hydrogen-bonded dimers. As expected, the H-bonding and π-π stacking plays a crucial role in structure modification [13,14,59–63]. The presence of methanol in the structure does not show any disorder in the crystal structure, probably due to its coordination in the crystal lattice only.

The second type of non-covalent interactions observed in the molecule is π-π interactions, which are observed between rings containing π-orbitals; those usually exist between two molecules with relatively "electron-rich/electron deficient" rings of the coordinated ligand. As observed in Figure 2b, highly pronounced π-π stacking exists between the rings with the shortest and longest C-C interplanar distances of two rings of 3.481 Å and 3.765 Å, respectively (Figure 2b). These intermolecular interactions give rise to layer formation for the molecule as discussed above and shown in Figure S2a,b. The π-π interaction has great importance in tuning and prediction of crystal structures.

The information gained from crystal structures on the covalent metal–ligand bond distances and angles has often other advantages on how the complexes or coordination ligands are packed in the crystal lattice. The effect of π-π interactions exhibit similar characteristics with those of hydrogen bonding on the crystal packing and then on the magnetic properties of the molecule. It is known that six-coordinated cobalt complexes are always more stable than with other geometries [50,64–66]. From this viewpoint, six-coordinated cobalt SIMs are promising for achieving a nice workable device in the future [67–69]. The π-π interactions enhance the conformational stability for the molecule and may provide chances of intermolecular electron transfer among the system so as to enhance or retard the magnetic property of the molecule.

The shortest and longest intralayer or the intrachain Co . . . Co distances are between the two adjacent molecules and are nonequivalent (7.034 Å and 7.415 Å, respectively) for the molecule with alternatively packed layers along the b axis in an ellipsoid configuration as depicted in Figure S3, indicating that the metal centers in a unit cell packed structure has less probability to interact each other through hydrogen bonding and π-π interactions. This property is very good to have appreciable magnetic properties for the molecule.

2.2. Magnetic Data

DC magnetic data was taken at $B = 0.1$ T. Raw magnetic data has been corrected for the underlying diamagnetism and presented as the temperature dependence of the effective magnetic moment (Figure 3). Its room temperature $\mu_{\text{eff}} = 4.67\ \mu_{\text{B}}$ is typical for an $S = 3/2$ spin system. On cooling, it adopts a value of $\mu_{\text{eff}} = 3.70\ \mu_{\text{B}}$ at $T = 2.0$ K, which is a fingerprint of zero-field splitting. The magnetization per formula unit at $T = 2.0$ K and $B = 7.0$ T adopts a value $M_1 = M_{\text{mol}}/(N_A \mu_{\text{B}}) = 2.63$, which is smaller than the hypothetical spin-free value of 3.0 again due to the zero-field splitting. The DC susceptibility and magnetization data was fitted simultaneously by employing the spin Hamiltonian that includes the axial zero-field splitting parameter D.

$$\hat{H}_k = D(\hat{S}_z^2 - \vec{S}^2/3)\hbar^{-2} + \mu_{\text{B}}B(g_z\hat{S}_z\cos\vartheta_k + g_x\hat{S}_x\sin\vartheta_k)\hbar^{-1}$$

The Zeeman term has been applied in 16 directions of the magnetic field along a quarter of meridian and the resulting magnetic susceptibility and/or magnetization was averaged in order to mimic the situation in the powder sample. Results of the fitting procedure are represented by solid lines in Figure 3. In match with the theoretical predictions, the D-parameter adopts a positive value for the compressed tetragonal bipyramid of the $\{CoO_4N_2\}$ chromophore: $D/hc = 29.6\text{cm}^{-1}$. Whereas the fit of the susceptibility is almost perfect, theoretical magnetization at higher fields declines from the experimental one. One of the reasons could originate in the fact that the solid-state sample contains two different

units with different distortion from the ideal tetragonal bipyramid. A small van Vleck correction χ_{TIM} compensates the uncertainty in the underlying diamagnetism and some temperature-independent paramagnetism.
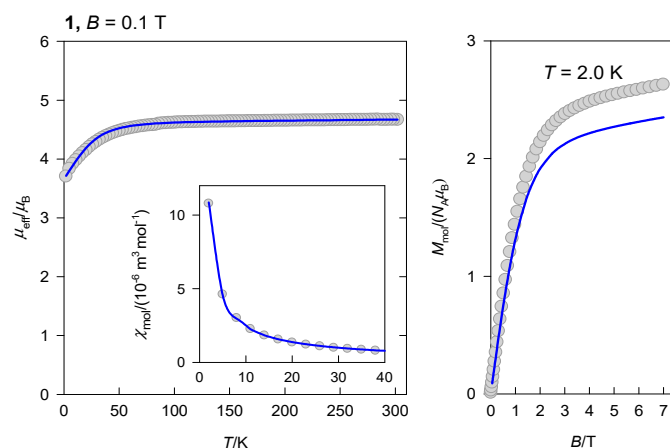
Figure 3. Left: temperature dependence of the effective magnetic moment; inset-molar magnetic susceptibility; right-field dependence of the magnetization. Lines–fitted with $D/hc = 29.6$ cm^{-1}, $g_x = 2.49$, $g_z = 2.12$, $\chi_{TIM} = 2.7 \times 10^{-9}$ m^3 mol^{-1} [SI].

The AC susceptibility data was scanned first for a set of trial frequencies of the oscillating field $B_{AC} = 0.35$ mT at $T = 2.0$ K and ramping the external magnetic field. At zero fields, the out-of-phase susceptibility is silent. However, with increasing B_{DC}, the χ'' component passes through a maximum and then attenuates (Figure 4). This is a feature of the slow magnetic relaxation that is supported by the external magnetic field.
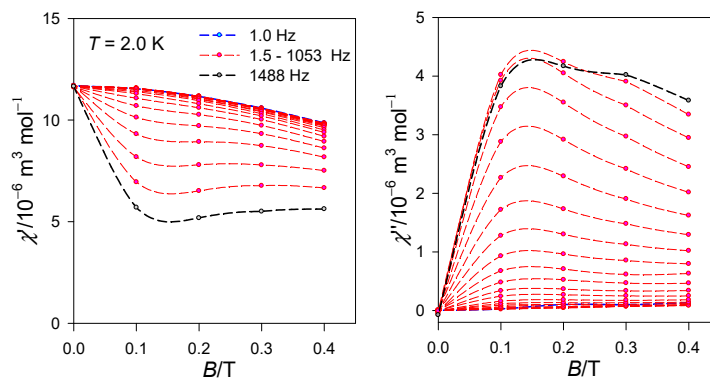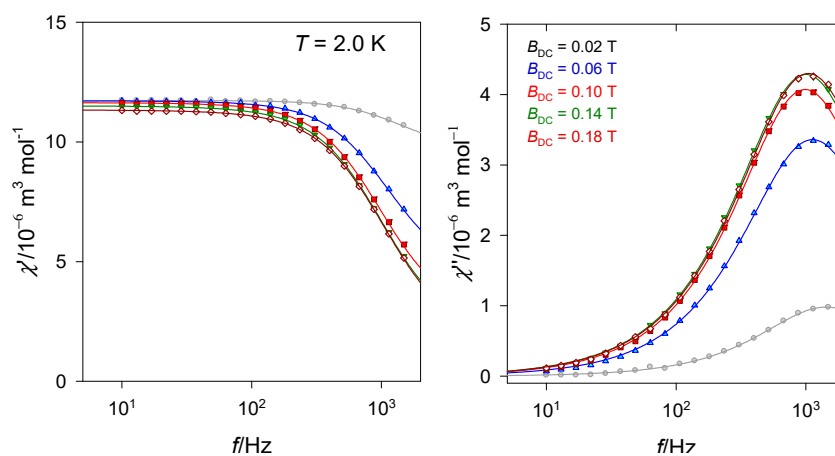

Figure 4. Field dependence of the AC susceptibility for **1** for a set of frequencies at T = 2.0 K.

A field effect of the AC susceptibility is presented in Figure 5. It clearly can be seen that the maximum of the out-of-phase susceptibility culminates at the frequency of 1000 Hz and the external field $B_{DC} = 0.02$–0.18 T. The in-phase and the out-of-phase susceptibility were fitted simultaneously to the extended Debye model and the obtained parameters (the adiabatic susceptibility χ_S, the isothermal susceptibility χ_T, the distribution parameter α, and the relaxation time (τ) were used in reconstructing the solid line that passes tightly through the discrete experimental points).
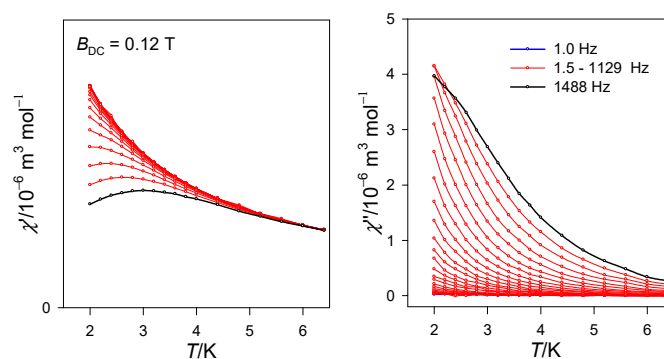
Temperature evolution of the AC susceptibility components is presented at Figure 6. It can be seen that the in-phase susceptibilities for different frequencies merge at $T \sim 6.5$ K; at the same temperature, the out-of-phase component vanishes. This is the temperature at which the substance turns to the ordinary paramagnetic phase.

The same data-set has been rearranged in Figure 7 where the AC susceptibility components are plotted as a function of the frequency f of the oscillating field for a set of
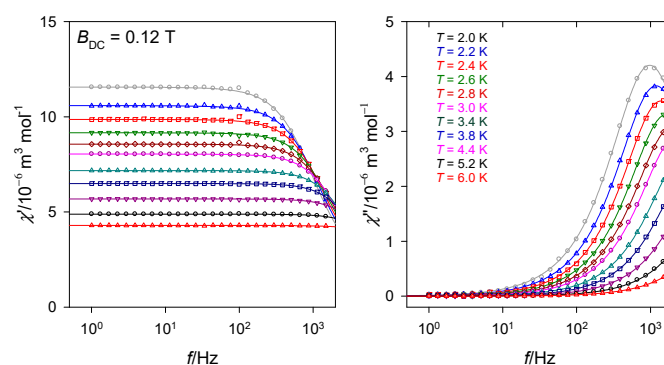
temperatures; everything at the selected external field B_{DC} = 0.12 T. The relaxation time for the single-mode relaxation process is τ = 0.16(1) ms at T = 2.0 K and B_{DC} = 0.12 T.

Figure 5. Frequency dependence of the AC susceptibility for **1** for a set of external fields at T = 2.0 K.
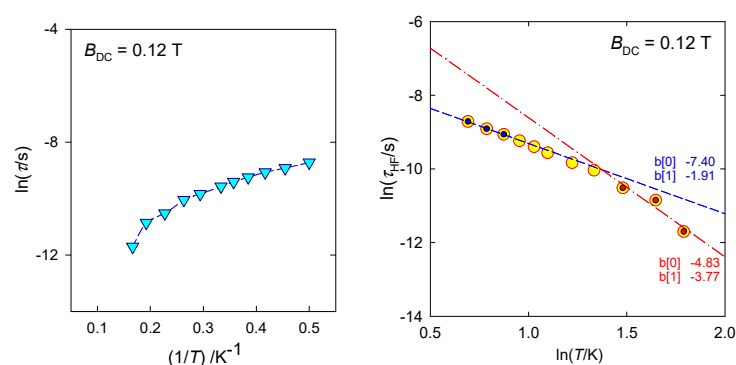

Figure 6. Temperature dependence of the AC susceptibility for **1** for a set of external fields at B_{DC} = 0.12 T.

Figure 7. Frequency dependence of the AC susceptibility for **1** for a set of temperatures at B_{DC} = 0.12 T.

Arrhenius-like plot $\ln\tau$ vs. T^{-1} is shown in Figure 8. It shows, with expectations, a decrease of the relaxation time on heating. The same data-set is used in the right panel where three low-temperature and high-temperature points were fitted by a straight line: $\ln\tau^{-} = b_{[0]} + b_{[1]}\ln T$. This allows subtracting the temperature coefficient $\tau^{-1} = CT^{n}$: n(LT) = 1.9 suggests a direct relaxation mechanism (close to its hindered modification called the phonon-bottleneck effect), whereas n(HT) = 3.8 and tends to approach the value typical for the Raman relaxation process.

Figure 8. Temperature dependence of the relaxation time for the molecule.

3. Materials and Methods

$CoCl_2 \bullet 6H_2O$, 5-bromo-vanillin, 4-aminoantipyrine, methanol, triethylamine and ethanol were used for the synthesis. All chemicals were commercially available and used as received. The crystal structure was obtained from single crystal X-ray analysis. The magnetic susceptibility measurements were performed with a Quantum Design MPMS XL-7 SQUID magnetometer between 2 and 300 K on a polycrystalline sample of 30 mg mixed with eicosane. The data were corrected for diamagnetic contributions of all components.

3.1. Synthesis $Co(C_{19}H_{17}BrN_3O_3)_2 \cdot 4CH_3OH$ (**1**)

The complex **1** was prepared by the addition of $CoCl_2 \bullet 6H_2O$ (0.1 mmol, 0.0238 g) in 10 mL methanol to a mixture of 5-bromo-vanillin (1.0 mmol, 0.231 g) in 5 mL methanol and 4-aminoantipyrine (1.0 mmol, 0.203 g) in 5 mL methanol in the presence of 2 drops of triethylamine. The resultant solution was refluxed for 2 h as in Scheme 1. It was then cooled and filtered. The crystals suitable for X-ray diffraction analysis were separated as orange to red blocks by slow evaporation in three weeks. The yield, 0.724 g, 75%. CHN calculated (%) for $C_{42}H_{50}Br_2CoN_6O_{10}$ (**1**) C, 49.5, H, 4.9, N, 8.2, Co, 5.7 found (%) C, 48.9, H, 4.7, N, 8.1, Co, 5.5, IR cm^{-1} (KBr); 3477(s), 2924(m), 1630 (s), 1583(s), 867(s),504(s), 463(m).
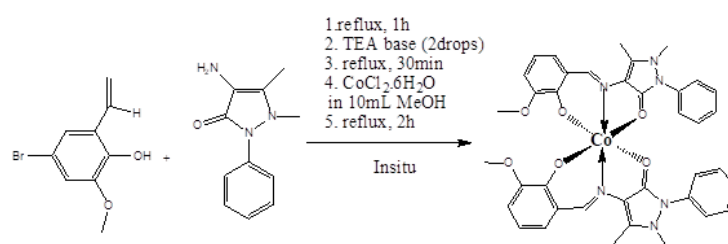
Scheme 1. Synthesis of the complex **1**.

3.2. Physical Measurements

DC measurement was performed on a polycrystalline sample mixed with eicosane between 300–2 K using a SQUID MPMS-XL magnetometer. A small field B_{DC} = 0.1 T has been applied in taking the temperature dependence of the static magnetic susceptibility between T = 2–350 K. These data was corrected for the underlying diamagnetism. Alternating current (ac) magnetic susceptibility measurements were performed in the temperature range of 2.0–6.5 K under variable applied static fields.

3.3. X-ray Crystallography

X-ray diffraction data of single crystals was collected on a STOE Stradivari X-ray diffractometer equipped with a variable-temperature nitrogen cold stream using GaK\α radiation (λ = 1.34143 Å) using a mirror monochromator at 160 K (Table S1). Crystal parameters and refinement results for the compound are summarized in Table S1. The structure was solved by standard direct methods and subsequently completed by Fourier

recycling by using the SHELXTL software packages. The obtained model was refined with SHELXL against F^2 on all data by full-matrix least squares. In the molecule, all non-hydrogen atoms were refined anisotropically. The graphical manipulation was performed with the Olex2 and Mercury program.

4. Conclusions

In a nutshell, we have synthesized and characterized mononuclear cobalt(II) complex with a Schiff base ligand formed from 5-bromo-vanillin and 4-aminoantipyrine, which exhibits field-induced, slow magnetic relaxation. Single crystal XRD studies reveal that the ligand coordinates to the metal ion through carbonyl oxygen of the amino moiety and deprotonated hydroxyl group from aldehyde part and the azomethine nitrogen, out of two ligand motifs, generating compressed tetragonal bipyramidal coordination geometry around Co(II) ion. The presence of benzene rings in the ligand not only effectively tune the coordination environment but also dramatically facilitates the crystal packing through various weaker non-covalent forces through H-bonding and π-π interactions. This study has initiated our aim of opening up more monomeric low-valent complexes with first row transition metals, exhibiting superior SMM characteristics with Schiff base ligands.

Supplementary Materials: The following supporting information can be downloaded at: https://www.mdpi.com/article/10.3390/inorganics10080105/s1, Figure S1: Crystal packing along b axis (a) without H-bonding (b) with H-bonding; Figure S2: Crystal packing along b axis (a) without H-bonding (b) with H-bonding; Figure S3: Intralayer M...M distances in the molecule; Table S1: Crystal data and structure refinement for $Co(C_{19}H_{17}BrN_3O_3)_2$; Table S2: Selected bond Lengths for $Co(C_{19}H_{17}BrN_3O_3)_2$; Table S3. Selected bond angles for $Co(C_{19}H_{17}BrN_3O_3)$.

References

1. Affronte, M. Molecular Nanomagnets for Information Technologies. *J. Mater. Chem.* **2009**, *19*, 1731–1737. [CrossRef]
2. Lumetti, S.; Candini, A.; Godfrin, C.; Balestro, F.; Wernsdorfer, W.; Klyatskaya, S.; Ruben, M.; Affronte, M. Single-Molecule Devices with Graphene Electrodes. *Dalton Trans.* **2016**, *45*, 16570–16574. [CrossRef]
3. Shao, D.; Shi, L.; Wei, H.Y.; Wang, X.Y. Field-Induced Single-Ion Magnet Behaviour in Two New Cobalt(II) Coordination Polymers with 2,4,6-Tris(4-Pyridyl)-1,3,5-Triazine. *Inorganics* **2017**, *5*, 90. [CrossRef]
4. Kar, P.; Biswas, R.; Drew, M.G.B.; Ida, Y.; Ghosh, A. Structure and Magnetic Properties of an Unprecedented Syn-Anti l-Nitrito-1kO:2kO′ Bridged Mn(III)-Salen Complex and Its Isoelectronic and Isostructural Formate Analogue. *Dalton Trans.* **2011**, *40*, 3295–3304. [CrossRef] [PubMed]
5. Kharwar, A.K.; Mondal, A.; Sarkar, A.; Rajaraman, G.; Konar, S. Modulation of Magnetic Anisotropy and Exchange Interaction in Phenoxide-Bridged Dinuclear Co(II) Complexes. *Inorg. Chem.* **2021**, *60*, 11948–11956. [CrossRef]

6.   Kazin, P.E.; Zykin, M.A.; Trusov, L.A.; Eliseev, A.A.; Magdysyuk, O.V.; Dinnebier, R.E.; Kremer, R.K.; Felser, C.; Jansen, M. A Co-Based Single-Molecule Magnet Confined in a Barium Phosphate Apatite Matrix with a High Energy Barrier for Magnetization Relaxation. *Chem. Commun.* **2017**, *53*, 5416–5419. [CrossRef]

7.   Milios, C.J.; Winpenny, R.E.P. Cluster-Based Single-Molecule Magnets. *Struct. Bond.* **2015**, *164*, 1–109. [CrossRef]

8.   Rechkemmer, Y.; Breitgoff, F.D.; Van Der Meer, M.; Atanasov, M.; Hakl, M.; Orlita, M.; Neugebauer, P.; Neese, F.; Sarkar, B.; Van Slageren, J. A Four-Coordinate Cobalt(II) Single-Ion Magnet with Coercivity and a Very High Energy Barrier. *Nat. Commun.* **2016**, *7*, 10467. [CrossRef]

9.   Campbell, V.E.; Tonelli, M.; Cimatti, I.; Moussy, J.B.; Tortech, L.; Dappe, Y.J.; Rivière, E.; Guillot, R.; Delprat, S.; Mattana, R.; et al. Engineering the Magnetic Coupling and Anisotropy at the Molecule-Magnetic Surface Interface in Molecular Spintronic Devices. *Nat. Commun.* **2016**, *7*, 13646. [CrossRef]

10.   Coronado, E. Molecular Magnetism: From Chemical Design to Spin Control in Molecules, Materials and Devices. *Nat. Rev. Mater.* **2020**, *5*, 87–104. [CrossRef]

11.   Shao, D.; Wang, X.Y. Development of Single-Molecule Magnets†. *Chin. J. Chem.* **2020**, *38*, 1005–1018. [CrossRef]

12.   Shen, Y.; Ito, H.; Zhang, H.; Yamochi, H.; Cosquer, G.; Herrmann, C.; Ina, T.; Yoshina, S.K.; Breedlove, B.K.; Otsuka, A.; et al. Emergence of Metallic Conduction and Cobalt(II)-Based Single-Molecule Magnetism in the Same Temperature Range. *J. Am. Chem. Soc.* **2021**, *143*, 4891–4895. [CrossRef] [PubMed]

13.   Novitchi, G.; Jiang, S.; Shova, S.; Rida, F.; Hlavička, I.; Orlita, M.; Wernsdorfer, W.; Hamze, R.; Martins, C.; Suaud, N.; et al. From Positive to Negative Zero-Field Splitting in a Series of Strongly Magnetically Anisotropic Mononuclear Metal Complexes. *Inorg. Chem.* **2017**, *56*, 14809–14822. [CrossRef] [PubMed]

14.   Jin, X.X.; Chen, X.X.; Xiang, J.; Chen, Y.Z.; Jia, L.H.; Wang, B.W.; Cheng, S.C.; Zhou, X.; Leung, C.F.; Gao, S. Slow Magnetic Relaxation in a Series of Mononuclear 8-Coordinate Fe(II) and Co(II) Complexes. *Inorg. Chem.* **2018**, *57*, 3761–3774. [CrossRef]

15.   Dolai, M.; Mondal, A.; Liu, J.L.; Ali, M. Three Novel Mononuclear Mn(III)-Based Magnetic Materials with Square Pyramidal: Versus Octahedral Geometries. *New J. Chem.* **2017**, *41*, 10890–10898. [CrossRef]

16.   Luo, Q.C.; Zheng, Y.Z. Methods and Models of Theoretical Calculation for Single-Molecule Magnets. *Magnetochemistry* **2021**, *7*, 107. [CrossRef]

17.   Zadrozny, J.M.; Telser, J.; Long, J.R. Slow Magnetic Relaxation in the Tetrahedral Cobalt(II) Complexes [Co(EPh)4]2- (EO, S, Se). *Polyhedron* **2013**, *64*, 209–217. [CrossRef]

18.   El-Khatib, F.; Cahier, B.; Shao, F.; López-Jordà, M.; Guillot, R.; Rivière, E.; Hafez, H.; Saad, Z.; Girerd, J.J.; Guihéry, N.; et al. Design and Magnetic Properties of a Mononuclear Co(II) Single Molecule Magnet and Its Antiferromagnetically Coupled Binuclear Derivative. *Inorg. Chem.* **2017**, *56*, 4601–4608. [CrossRef]

19.   Gomez-Coca, S.; Cremades, E.; Aliaga-Alcalde, N.; Ruiz, E. Mononuclear Single-Molecule Magnets: Tailoring the Magnetic Anisotropy of First-Row Transition-Metal Complexes. *J. Am. Chem. Soc.* **2013**, *135*, 7010–7018. [CrossRef]

20.   Gebrezgiabher, M.; Bayeh, Y.; Gebretsadik, T. Lanthanide-Based Single-Molecule Magnets Derived from Schiff Base Ligands of Salicylaldehyde Derivatives. *Inorganics* **2020**, *8*, 66. [CrossRef]

21.   Villa-Pérez, C.; Oyarzabal, I.; Echeverría, G.A.; Valencia-Uribe, G.C.; Seco, J.M.; Soria, D.B. Single-Ion Magnets Based on Mononuclear Cobalt (II) Complexes with Sulfadiazine. *Eur. J. Inorg. Chem.* **2016**, *29*, 4835–4841. [CrossRef]

22.   Senthil Kumar, K.; Bayeh, Y.; Gebretsadik, T.; Elemo, F.; Gebrezgiabher, M.; Thomas, M.; Ruben, M. Spin-Crossover in Iron(II)-Schiff Base Complexes. *Dalton Trans.* **2019**, *48*, 15321–15337. [CrossRef] [PubMed]

23.   Zadrozny, J.M.; Xiao, D.J.; Atanasov, M.; Long, G.J.; Grandjean, F.; Neese, F.; Long, J.R. Magnetic Blocking in a Linear Iron(I) Complex. *Nat. Chem.* **2013**, *5*, 577–581. [CrossRef]

24.   Fataftah, M.S.; Zadrozny, J.M.; Rogers, D.M.; Freedman, D.E. A Mononuclear Transition Metal Single-Molecule Magnet in a Nuclear Spin-Free Ligand Environment. *Inorg. Chem.* **2014**, *53*, 10716–10721. [CrossRef]

25.   Frost, J.M.; Harriman, K.L.M.; Murugesu, M. The Rise of 3-d Single-Ion Magnets in Molecular Magnetism: Towards Materials from Molecules? *Chem. Sci.* **2016**, *7*, 2470–2491. [CrossRef]

26.   Mondal, A.K.; Sundararajan, M.; Konar, S. A New Series of Tetrahedral Co(II) Complexes [CoLX2] (X = NCS, Cl, Br, I) Manifesting Single-Ion Magnet Features. *Dalton Trans.* **2018**, *47*, 3745–3754. [CrossRef] [PubMed]

27.   Lan, W.; Hao, X.; Dou, Y.; Zhou, Z.; Yang, L.; Liu, H.; Li, D.; Dong, Y.; Kong, L.; Zhang, D. Various Structural Types of Cyanide-Bridged Fe^{III}–Mn^{III} Bimetallic Coordination Polymers (CPs) and Polynuclear Clusters Based-on A New *mer*-Tricyanoiron(III)Building Block: Synthesis, Crystal Structures, and Magnetic Properties. *Polymers* **2019**, *11*, 1585. [CrossRef]

28.   Hay, M.A.; Sarkar, A.; Marriott, K.E.R.; Wilson, C.; Rajaraman, G.; Murrie, M. Investigation of the Magnetic Anisotropy in a Series of Trigonal Bipyramidal Mn(Ii) Complexes. *Dalton Trans.* **2019**, *48*, 15480–15486. [CrossRef]

29.   Perlepe, P.S.; Maniaki, D.; Pilichos, E.; Katsoulakou, E.; Perlepes, S.P. Smart Ligands for Efficient 3d-, 4d- and 5d-Metal Single-Molecule Magnets and Single-Ion Magnets. *Inorganics* **2020**, *8*, 39. [CrossRef]

30.   Huang, X.C.; Zhou, C.; Shao, D.; Wang, X.Y. Field-Induced Slow Magnetic Relaxation in Cobalt(II) Compounds with Pentagonal Bipyramid Geometry. *Inorg. Chem.* **2014**, *53*, 12671–12673. [CrossRef]

31.   Gebrezgiabher, M.; Schlittenhardt, S.; Rajnák, C.; Sergawie, A.; Ruben, M.; Thomas, M.; Boča, R. A Tetranuclear Dysprosium Schiff Base Complex Showing Slow Relaxation of Magnetization. *Inorganics* **2022**, *10*, 66. [CrossRef]

32.   Mondal, A.K.; Goswami, T.; Misra, A.; Konar, S. Probing the Effects of Ligand Field and Coordination Geometry on Magnetic Anisotropy of Pentacoordinate Cobalt(II) Single-Ion Magnets. *Inorg. Chem.* **2017**, *56*, 6870–6878. [CrossRef] [PubMed]

33. Shao, D.; Zhang, S.L.; Shi, L.; Zhang, Y.Q.; Wang, X.Y. Probing the Effect of Axial Ligands on Easy-Plane Anisotropy of Pentagonal-Bipyramidal Cobalt(II) Single-Ion Magnets. *Inorg. Chem.* **2016**, *55*, 10859–10869. [CrossRef] [PubMed]

34. Habib, F.; Luca, O.R.; Vieru, V.; Shiddiq, M.; Korobkov, I.; Gorelsky, S.I.; Takase, M.K.; Chibotaru, L.F.; Hill, S.; Crabtree, R.H.; et al. Influence of the Ligand Field on Slow Magnetization Relaxation versus Spin Crossover in Mononuclear Cobalt Complexes. *Angew. Chem.-Int. Ed.* **2013**, *52*, 11290–11293. [CrossRef]

35. Peng, Y.; Mereacre, V.; Anson, C.E.; Zhang, Y.; Bodenstein, T.; Fink, K.; Powell, A.K. Field-Induced Co(II) Single-Ion Magnets with Mer-Directing Ligands but Ambiguous Coordination Geometry. *Inorg. Chem.* **2017**, *56*, 6056–6066. [CrossRef]

36. Chen, L.; Dulaney, H.A.; Wilkins, B.O.; Farmer, S.; Zhang, Y.; Fronczek, F.R.; Jurss, J.W. High-Spin Enforcement in First-Row Metal Complexes of a Constrained Polyaromatic Ligand: Synthesis, Structure, and Properties. *New J. Chem.* **2018**, *42*, 18667–18677. [CrossRef]

37. Li, G.L.; Sato, O. A Compressed Octahedral Cobalt(II) Complex in the Crystal Structure of Diaqua[6,6′-Sulfanediylbis(2,2′-Bipyridine)]Cobalt(II) Dinitrate Li Guo-Ling. *Acta Crystallogr. Sect. E Crystallogr. Commun.* **2017**, *73*, 993–995. [CrossRef]

38. Madhu, N.T.; Tang, J.K.; Hewitt, I.J.; Clérac, R.; Wernsdorfer, W.; Van Slageren, J.; Anson, C.E.; Powell, A.K. What Makes a Single Molecule Magnet? *Polyhedron* **2005**, *24*, 2864–2869. [CrossRef]

39. Goswami, S.; Mondal, A.K.; Konar, S. Nanoscopic Molecular Magnets. *Inorg. Chem. Front.* **2015**, *2*, 687–712. [CrossRef]

40. Bu, X.H.; Morishita, H.; Tanaka, K.; Biradha, K.; Furusho, S.; Shionoya, M. A Spontaneously Resolved Chiral Molecular Box: A Cyclic Tetranuclear Zn(II) Complex with DPTZ (DPTZ = 3,6-Di-2-Pyridyl-1,2,4,5-Tetrazine). *Chem. Commun.* **2000**, 971–972. [CrossRef]

41. Xie, L.; Wei, Y.; Wang, Y.; Hou, H.; Fan, Y.; Zhu, Y. 2D and 3D Binuclear Cobalt Supramolecular Complexes: Synthesis and Crystal Structures. *J. Mol. Struct.* **2004**, *692*, 201–207. [CrossRef]

42. Nikam, R.; Rayaprol, S.; Mukherjee, S.; Kaushik, S.D.; Goyal, P.S.; Babu, P.D.; Radha, S.; Siruguri, V. Structure and Magnetic Properties of Mn Doped α-Fe$_2$O$_3$. *Phys. B Condens. Matter* **2019**, *574*, 411663. [CrossRef]

43. Moseley, I.P.; Lin, C.Y.; Zee, D.Z.; Zadrozny, J.M. Synthesis and Magnetic Characterization of a Dinuclear Complex of Low-Coordinate Iron(II). *Polyhedron* **2020**, *175*, 114171. [CrossRef] [PubMed]

44. Hay, M.A.; Sarkar, A.; Craig, G.A.; Bhaskaran, L.; Nehrkorn, J.; Ozerov, M.; Marriott, K.E.R.; Wilson, C.; Rajaraman, G.; Hill, S.; et al. In-Depth Investigation of Large Axial Magnetic Anisotropy in Monometallic 3d Complexes Using Frequency Domain Magnetic Resonance and: Ab Initio Methods: A Study of Trigonal Bipyramidal Co(Ii). *Chem. Sci.* **2019**, *10*, 6354–6361. [CrossRef] [PubMed]

45. Mondal, A.K.; Mondal, A.; Konar, S. Field Induced Single Ion Magnetic Behaviour in Square-Pyramidal Cobalt(II) Complexes with Easy-Plane Magnetic Anisotropy. *Magnetochemistry* **2019**, *5*, 27–33. [CrossRef]

46. Murrie, M. Cobalt(Ii) Single-Molecule Magnets. *Chem. Soc. Rev.* **2010**, *39*, 1986–1995. [CrossRef]

47. Shao, F.; Cahier, B.; Wang, Y.T.; Yang, F.L.; Rivière, E.; Guillot, R.; Guihéry, N.; Tong, J.P.; Mallah, T. Magnetic Relaxation Studies on Trigonal Bipyramidal Cobalt(II) Complexes. *Chem.-Asian J.* **2020**, *15*, 391–397. [CrossRef]

48. Gómez-Coca, S.; Urtizberea, A.; Cremades, E.; Alonso, P.J.; Camón, A.; Ruiz, E.; Luis, F. Origin of Slow Magnetic Relaxation in Kramers Ions with Non-Uniaxial Anisotropy. *Nat. Commun.* **2014**, *5*, 4300. [CrossRef]

49. Singh, S.K.; Rajaraman, G. Probing the Origin of Magnetic Anisotropy in a Dinuclear {Mn IIICuII} Single-Molecule Magnet: The Role of Exchange Anisotropy. *Chem.-A Eur. J.* **2014**, *20*, 5214–5218. [CrossRef]

50. Vallejo, J.; Castro, I.; Ruiz-García, R.; Cano, J.; Julve, M.; Lloret, F.; De Munno, G.; Wernsdorfer, W.; Pardo, E. Field-Induced Slow Magnetic Relaxation in a Six-Coordinate Mononuclear Cobalt(II) Complex with a Positive Anisotropy. *J. Am. Chem. Soc.* **2012**, *134*, 15704–15707. [CrossRef]

51. Vallejo, J.; Viciano-Chumillas, M.; Lloret, F.; Julve, M.; Castro, I.; Krzystek, J.; Ozerov, M.; Armentano, D.; De Munno, G.; Cano, J. Coligand Effects on the Field-Induced Double Slow Magnetic Relaxation in Six-Coordinate Cobalt(II) Single-Ion Magnets (SIMs) with Positive Magnetic Anisotropy. *Inorg. Chem.* **2019**, *58*, 15726–15740. [CrossRef]

52. Świtlicka, A.; Palion-Gazda, J.; Machura, B.; Cano, J.; Lloret, F.; Julve, M. Field-Induced Slow Magnetic Relaxation in Pseudoocta-hedral Cobalt(Ii) Complexes with Positive Axial and Large Rhombic Anisotropy. *Dalton Trans.* **2019**, *48*, 1404–1417. [CrossRef] [PubMed]

53. Pilichos, E.; Font-Bardia, M.; Cano, J.; Escuer, A.; Mayans, J. Slow Magnetic Relaxation for Cobalt (II) Complexes in Axial Bipyramidal Environment: An $S = \frac{1}{2}$ Spin Case. *Dalton Trans.* **2022**, *51*, 8986–8993. [CrossRef] [PubMed]

54. Yao, B.; Deng, Y.F.; Li, T.; Xiong, J.; Wang, B.W.; Zheng, Z.; Zhang, Y.Z. Construction and Magnetic Study of a Trigonal-Prismatic Cobalt(II) Single-Ion Magnet. *Inorg. Chem.* **2018**, *57*, 14047–14051. [CrossRef] [PubMed]

55. Fürmeyer, F.; Münzberg, D.; Carrella, L.M.; Rentschler, E. First Cobalt(II) Spin Crossover Compound with N4S2-Donorset. *Molecules* **2020**, *25*, 855. [CrossRef]

56. Pankratova, Y.A.; Nelyubina, Y.V.; Novikov, V.V.; Pavlov, A.A. High-Spin Cobalt(II) Complex with Record-Breaking Anisotropy of the Magnetic Susceptibility According to Paramagnetic NMR Spectroscopy Data. *Russ. J. Coord. Chem. Koord. Khimiya* **2021**, *47*, 10–16. [CrossRef]

57. Jia, H.R.; Li, J.; Sun, Y.X.; Guo, J.Q.; Yu, B.; Wen, N.; Xu, L. Two Supramolecular Cobalt(II) Complexes: Syntheses, Crystal Structures, Spectroscopic Behaviors, and Counter Anion Effects. *Crystals* **2017**, *7*, 247. [CrossRef]

58. Dutta, D.; Nashre-ul-Islam, S.M.; Saha, U.; Frontera, A.; Bhattacharyya, M.K. Cu(II) and Co(II) Coordination Solids Involving Unconventional Parallel Nitrile(π)-nitrile(π) and Energetically Significant Cooperative Hydrogen Bonding Interactions: Experimental and Theoretical Studies. *J. Mol. Struct.* **2019**, *1195*, 733–743. [CrossRef]

59. Li, H.; Zhang, S.G.; Xie, L.M.; Yu, L.; Shi, J.M. π-π Stacking, Hydrogen Bonding and Anti-Ferromagnetic Coupling Mechanism on a Mononuclear Cu(II) Complex. *J. Coord. Chem.* **2011**, *64*, 1456–1468. [CrossRef]

60. Tang, J.; Costa, J.S.; Smulders, S.; Molnár, G.; Bousseksou, A.; Teat, S.J.; Li, Y.; Van Albada, G.A.; Gamez, P.; Reedijk, J. Two-Step Spin-Transition Iron(III) Compound with a Wide [High Spin-Low Spin] Plateau. *Inorg. Chem.* **2009**, *48*, 2128–2135. [CrossRef]

61. Wheeler, S.E. Understanding Substituent Effects in Noncovalent Interactions Involving Aromatic Rings. *Acc. Chem. Res.* **2013**, *46*, 1029–1038. [CrossRef] [PubMed]

62. Oshita, H.; Suzuki, T.; Kawashima, K.; Abe, H.; Tani, F.; Mori, S.; Yajima, T.; Shimazaki, Y. The Effect of π-π Stacking Interaction of the Indole Ring with the Coordinated Phenoxyl Radical in a Nickel(II)-Salen Type Complex. Comparison with the Corresponding Cu(II) Complex. *Dalton Trans.* **2019**, *48*, 12060–12069. [CrossRef] [PubMed]

63. Rigamonti, L.; Bridonneau, N.; Poneti, G.; Tesi, L.; Sorace, L.; Pinkowicz, D.; Jover, J.; Ruiz, E.; Sessoli, R.; Cornia, A. A Pseudo-Octahedral Cobalt(II) Complex with Bispyrazolylpyridine Ligands Acting as a Zero-Field Single-Molecule Magnet with Easy Axis Anisotropy. *Chem.-A Eur. J.* **2018**, *24*, 8857–8868. [CrossRef]

64. Comba, P.; Kerscher, M.; Lawrance, G.A.; Martin, B.; Wadepohl, H. Stable Five- and Six-Coordinate Cobalt (III) Complexes with a Pentadentate Bispidine Ligand. *Angew. Chem. Int. Ed.* **2008**, *47*, 4740–4743. [CrossRef] [PubMed]

65. Roy, S.; Oyarzabal, I.; Vallejo, J.; Cano, J.; Colacio, E.; Bauza, A.; Frontera, A.; Kirillov, A.M.; Drew, M.G.B.; Das, S. Two Polymorphic Forms of a Six-Coordinate Mononuclear Cobalt(II) Complex with Easy-Plane Anisotropy: Structural Features, Theoretical Calculations, and Field-Induced Slow Relaxation of the Magnetization. *Inorg. Chem.* **2016**, *55*, 8502–8513. [CrossRef]

66. Lloret, F.; Julve, M.; Cano, J.; Ruiz-García, R.; Pardo, E. Magnetic Properties of Six-Coordinated High-Spin Cobalt (II) Complexes: Theoretical Background and Its Application. *Inorg. Chim. Acta* **2008**, *361*, 3432–3445. [CrossRef]

67. Zhang, Y.Z.; Gómez-Coca, S.; Brown, A.J.; Saber, M.R.; Zhang, X.; Dunbar, K.R. Trigonal Antiprismatic Co(II) Single Molecule Magnets with Large Uniaxial Anisotropies: Importance of Raman and Tunneling Mechanisms. *Chem. Sci.* **2016**, *7*, 6519–6527. [CrossRef] [PubMed]

68. Hu, Z.B.; Jing, Z.Y.; Li, M.M.; Yin, L.; Gao, Y.D.; Yu, F.; Hu, T.P.; Wang, Z.; Song, Y. Important Role of Intermolecular Interaction in Cobalt(II) Single-Ion Magnet from Single Slow Relaxation to Double Slow Relaxation. *Inorg. Chem.* **2018**, *57*, 10761–10767. [CrossRef]

69. Chahine, A.Y.; Phonsri, W.; Murray, K.S.; Turner, D.R.; Batten, S.R. Coordination Polymers of a Bis-Isophthalate Bridging Ligand with Single Molecule Magnet Behaviour of the CoII Analogue. *Dalton Trans.* **2020**, *49*, 5241–5249. [CrossRef]